

## A New Stable High-Valent Diiron Center in R2 Mutant Y122H of *E. coli* Ribonucleotide Reductase Studied by High-Field EPR and $^{57}\text{Fe}$ -ENDOR

Matthias Kolberg,<sup>†</sup> Günther Bleifuss,<sup>†</sup> Stephan Pötsch,<sup>‡,§</sup> Astrid Gräslund,<sup>\*,‡</sup> Wolfgang Lubitz,<sup>†</sup> Günter Lassmann,<sup>†</sup> and Friedhelm Lendzian<sup>\*,†</sup>

Max-Volmer-Institut für Biophysikalische Chemie und Biochemie, Technische Universität Berlin, PC 14 Strasse des 17. Juni 135, D-10623 Berlin, Germany  
Department of Biophysics, Stockholm University Arrhenius Laboratories, S-10691 Stockholm, Sweden

Received February 18, 2000

The R2 subunit of ribonucleotide reductase (RNR), the rate limiting enzyme in DNA synthesis, contains an antiferromagnetically coupled  $\mu$ -oxo bridged diferric center and, in the active state, a stable tyrosyl radical at residue 122 in *E. coli*.<sup>1</sup> The diferric site and the tyrosyl radical can be generated from apo R2 in a reaction with molecular oxygen and  $\text{Fe}^{\text{II}}$ .<sup>2</sup> This reaction involves oxygen activation as in similar dinuclear iron enzymes such as methane monooxygenase (MMO)<sup>3c</sup> and has found considerable interest in recent years.<sup>3</sup> During this reaction in R2 a short-lived antiferromagnetically coupled intermediate state X is observed, which has been assigned to an  $\text{Fe}^{\text{III}}\text{Fe}^{\text{IV}}$  state on the basis of ENDOR and Mössbauer experiments.<sup>4</sup> This state subsequently oxidizes Y122 to its radical form in wild-type R2.

In this communication we describe a new unusually stable (two weeks at room temperature) paramagnetic diiron center, named "H", which has been detected and identified by EPR and ENDOR spectroscopy in *E. coli* mutant R2-Y122H. Center H is formed spontaneously with about 3% yield in R2-Y122H in contrast to the amino acid radicals in other R2-Y122 mutants<sup>5</sup> which are formed only by the standard reconstitution reaction.<sup>2</sup> So far it has not been possible to increase the yield of center H. However, since we have also obtained the EPR signal of center H in single crystals of R2-Y122H (data not shown), it can be ruled out that center H is a contamination from a different protein.

In X-band EPR a single line of width 2.2 mT is observed for center H below 40 K (Figure 1A) and in W-band all three principal  $g$ -tensor components are resolved (Figure 1C and Table 1).  $^{57}\text{Fe}$  substituted R2-Y122H exhibits a larger EPR line width of 4.3 mT at X-band (see Figure 1B) and a pronounced broadening of each of the three  $g$ -components at W-band (Figure 1D) which indicates that significant spin density is localized on iron. This is also reflected in the EPR saturation behavior shown in Figure 1 (insert); at  $T = 20$  K the EPR signal of center H is saturated at

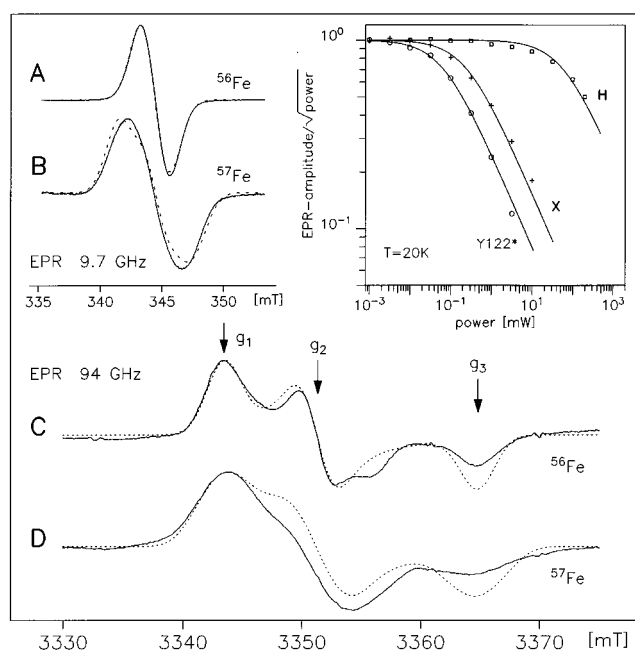


**Figure 1.** cw-EPR spectra of center H in *E. coli* RNR R2-Y122H. (A) X-band spectrum at  $T = 30$  K of  $^{56}\text{Fe}$  R2-Y122H (1.0 mM) and (B) of  $^{57}\text{Fe}$  R2-Y122H (0.9 mM); Bruker ESP 300E spectrometer, 1 mW microwave power ( $P_{\text{mw}}$ ), 12.5 kHz modulation frequency (mf), 0.7 mT modulation amplitude (ma). (C) W-band spectrum at  $T = 20$  K of  $^{56}\text{Fe}$  R2-Y122H (3.6 mM) and (D) of  $^{57}\text{Fe}$  R2-Y122H (3.0 mM); Bruker Elexsys 680E 94 GHz spectrometer,  $P_{\text{mw}} = 1.58$  mW, mf = 100 kHz, ma = 0.6 mT. Insert: X-band EPR microwave saturation at  $T = 20$  K of center H from R2-Y122H, intermediate X ( $\text{Fe}^{\text{III}}\text{Fe}^{\text{IV}}$ ) from R2-Y122F, and Y122\* from wild-type R2. Residual wild-type tyrosyl radical is suppressed by hydroxyurea, which had no effect on center H. Dotted traces: simulations with parameters from Table 1.

**Table 1.**  $g$  and  $^{57}\text{Fe}$  Hyperfine Data of Center H and Other Diiron Centers

paramagnetic center	$g$ -tensor	$^{57}\text{Fe}$ hyperfine tensors (MHz)			
center H in <i>E. coli</i>	2.0088(1)	72.5(2)	52.1(2)		
RNR R2-Y122H <sup>a</sup>	2.0040(1)	69.7(2)	Fe2 47.6(2)	Fe1	
	1.9960(2)	66.6(2)	45.1(2)		
intermediate X ( $\text{Fe}^{\text{III}}/\text{Fe}^{\text{IV}}$ )	2.007	-74.2	27.5		
in <i>E. coli</i> RNR R2-Y122F <sup>b,4</sup>	1.999	-72.2	Fe <sup>III</sup> 36.8	Fe <sup>IV</sup>	
	1.994	-73.2	36.8		
$\text{Fe}^{\text{II}}/\text{Fe}^{\text{III}}$ center in <i>M. cap-sulatus</i> MMO + dimethyl sulfoxide <sup>6</sup>	1.95	62	36		
	1.87	68	Fe <sup>III</sup> 38	Fe <sup>II</sup>	
	1.82	76	<20		

<sup>a</sup> Absolute values sorted by magnitude; numbers in parentheses are errors in the last digit. <sup>b</sup> Similar  $g$ -components of 2.011, 1.997, 1.986,<sup>13a</sup> and  $^{57}\text{Fe}$  hf tensor components of -64.5, -64.5, -64.5 MHz ( $\text{Fe}^{\text{III}}$ ), +36.5, +36.5, +20 MHz ( $\text{Fe}^{\text{IV}}$ )<sup>13b</sup> have been found for  $\text{Fe}^{\text{III}}\text{Fe}^{\text{IV}}$  model complexes.

2 orders of magnitude higher microwave power even than the  $\text{Fe}^{\text{III}}\text{Fe}^{\text{IV}}$  intermediate X. At higher temperatures ( $T > 80$  K) the spectrum is broadened beyond detection. The  $g$ -tensor values of center H are listed in Table 1 together with those of the  $\text{Fe}^{\text{II}}\text{Fe}^{\text{III}}$  center in MMO<sup>6</sup> and the  $\text{Fe}^{\text{III}}\text{Fe}^{\text{IV}}$  center in R2-Y122F (intermediate X)<sup>4</sup> and show good agreement with an  $\text{Fe}^{\text{III}}\text{Fe}^{\text{IV}}$  center.

The pulse ENDOR spectra of center H exhibit resonances from proton (12–18 MHz) and  $^{14}\text{N}$  nuclei (4–10 MHz) (Figure 2A,B) which will be analyzed in a forthcoming paper.<sup>7</sup> The weak broad

(6) DeRose, V. J.; Liu, K. E.; Lippard, S. J.; Hoffman, B. M. *J. Am. Chem. Soc.* 1996, 118, 121–134.

\* Author to whom correspondence should be addressed. E-mail: lendzian@echo.chem.tu-berlin.de or astrid@biophys.su.se.

<sup>†</sup> Technische Universität Berlin.

<sup>‡</sup> Stockholm University.

<sup>§</sup> Present address: Institute for Physiological Chemistry and Pathobiology, University of Mainz, D-55099 Mainz, Germany.

(1) Sjöberg, B.-M. *Struct. Bonding* 1997, 88, 139–173.

(2) Atkin, C. L.; Thelander, L.; Reichard, P.; Lang, G. *J. Biol. Chem.* 1973, 248, 7464–7472.

(3) (a) Solomon E. I.; Brunold, T. C.; Davis, M. I.; Kemsley, J. N.; Lee, S.-K.; Lehnert, N.; Neese, F.; Skulan, A. J.; Yang, Y.-S.; Zhou, J. *Chem. Rev.* 2000, 100, 235–349. (b) Andersson, K. K.; Gräslund, A. *Advances in Inorganic Chemistry*; Academic Press: Orlando, 1995; pp 359–408. (c) Wallar, B. J.; Lipscomb, J. D. *Chem. Rev.* 1996, 96, 2625–2658.

(4) Sturgeon, B. E.; Burdi, D.; Chen, S.; Huynh, B.-H.; Edmondson, D. E.; Stubbe, J.; Hoffman, B. M. *J. Am. Chem. Soc.* 1996, 118, 7551–7557.

(5) (a) Sahlin, M.; Lassmann, G.; Pötsch, S.; Sjöberg, B.-M.; Gräslund, A. *J. Biol. Chem.* 1995, 270, 12361–12372. (b) Lendzian, F.; Sahlin, M.; MacMillan, F.; Bittl, R.; Fiege, R.; Pötsch, S.; Sjöberg, B.-M.; Gräslund, A.; Lubitz, W.; Lassmann, G. *J. Am. Chem. Soc.* 1996, 118, 8111–8120. (c) Pötsch, S.; Lendzian, F.; Ingemarson, R.; Hörnberg, A.; Thelander, L.; Lubitz, W.; Lassmann, G.; Gräslund, A. *J. Biol. Chem.* 1999, 274, 17696–17704.

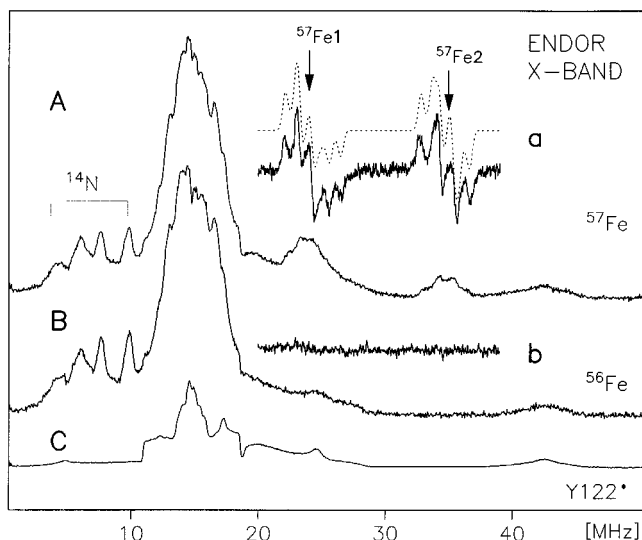


**Figure 2.** X-band Pulse Davies ENDOR spectra at  $T = 10$  K of center H in *E. coli* RNR R2-Y122H: (A)  $^{57}\text{Fe}$  R2-Y122H (2.1 mM), (B)  $^{56}\text{Fe}$  R2-Y122H (1.5 mM), and (C) Y122\* in wild-type R2 (1.0 mM); Bruker ESP 380E, microwave pulses 192, 96, 192 ns; radio frequency (rf) pulse 8  $\mu\text{s}$ ; accumulation time 10 h (A, B), 0.5 h (C). Inserts: X-band cw-ENDOR spectra (first derivative) at  $T = 8$  K of center H: (a) in  $^{57}\text{Fe}$  R2-Y122H and (b) in  $^{56}\text{Fe}$  R2-Y122H; Bruker ESP 300E,  $P_{\text{mw}} = 8$  mW,  $P_{\text{rf}} = 100$ –150 W,  $\text{mf} = 12.5$  kHz,  $\text{ma} = \pm 150$  kHz; accumulation time 3 h. Dotted trace: simulation, see text.

features near 26 and 42 MHz result from the Y122 radical in residual wild-type R2 (compare Figure 2C). In  $^{57}\text{Fe}$  substituted R2-Y122H two additional groups of lines appear around 25 and 35 MHz (Figure 2A). Each group consists of three pairs of peaks which are centered around the three  $^{57}\text{Fe}$  hyperfine (hf) tensor principal components ( $A_{1,2,3}/2$ ) and split by  $2\nu_{^{57}\text{Fe}}$  (0.9 MHz at X-band). All three components of the two  $^{57}\text{Fe}$  hf tensors have been obtained by simulation of the well-resolved continuous wave (cw)  $^{57}\text{Fe}$ -ENDOR spectrum (trace a in Figure 2A, Table 1).

The  $^{57}\text{Fe}$ -ENDOR results clearly show that center H is a *two-iron* site. The  $g$ -values near  $g \sim 2$  and the small hf anisotropy of  $^{57}\text{Fe}$  suggest an antiferromagnetically coupled diiron site with an  $S = 1/2$  ground state. To obtain information about the valence of the irons we compare the  $^{57}\text{Fe}$  hf tensors of center H with data from mixed valence diiron centers (Table 1). The larger  $^{57}\text{Fe}$  tensor of center H (Fe2 in Figure 2a) has similar components to those reported for  $\text{Fe}^{\text{III}}$  in both the  $\text{Fe}^{\text{III}}\text{Fe}^{\text{IV}}$  center of intermediate X<sup>4</sup> and in the  $\text{Fe}^{\text{II}}\text{Fe}^{\text{III}}$  of MMO,<sup>6</sup> and we therefore assign this tensor to  $\text{Fe}^{\text{III}}$ . The smaller  $^{57}\text{Fe}$  tensor assigned to  $\text{Fe}^{\text{IV}}$  in X<sup>4</sup> and to  $\text{Fe}^{\text{II}}$  in MMO<sup>6</sup> exhibits in both these cases a significant axial anisotropy, whereas the smaller  $^{57}\text{Fe}$  tensor of center H (Fe1 in Figure 2a) is more isotropic and the magnitude of its isotropic part is considerably larger than those of  $\text{Fe}^{\text{IV}}$  in X and  $\text{Fe}^{\text{II}}$  in MMO.

The  $^{57}\text{Fe}$  hf tensors (A) of antiferromagnetically coupled  $S = 5/2$  and 2 spin systems, like both the  $\text{Fe}^{\text{III}}\text{Fe}^{\text{II}}$  and the  $\text{Fe}^{\text{III}}\text{Fe}^{\text{IV}}$  in Table 1, are related to the intrinsic tensors ( $\mathbf{a}_i$ ) of the uncoupled irons by the spin projection factors  $7/3$  and  $-4/3$ , i.e.,  $\mathbf{A}(\text{Fe}^{\text{III}}) = 7/3\mathbf{a}_i(\text{Fe}^{\text{III}})$  and  $\mathbf{A}(\text{Fe}^{\text{IV}}) = -4/3\mathbf{a}_i(\text{Fe}^{\text{IV}})$ .<sup>4,8</sup> Considering the small anisotropy of both  $^{57}\text{Fe}$  hf tensors in center H we compare the isotropic traces of the respective tensors ( $A = (A_1 + A_2 + A_3)/3$ ;

(7) Pötsch, S.; Kolberg, M.; Bleifuss, G.; Logan, D.; Sjöberg, B.-M.; Gräslund, A.; Lubitz, W.; Lendzian, F.; Lassmann, G. Manuscript in preparation.

(8) Ravi, N.; Bollinger, J. M.; Huynh, B. H.; Edmondson, D. E.; Stubbe, J. J. Am. Chem. Soc. **1994**, *116*, 8007–8014.

$a_i = (a_{i1} + a_{i2} + a_{i3})/3$ ). The obtained intrinsic value for the larger  $^{57}\text{Fe}$  tensor ( $\text{Fe}^{\text{III}}$ ) in center H,  $|a_i| = 29.8$  MHz, agrees well with the values reported for Fe sites with octahedral coordination (–28 to –30 MHz) and also with the value reported for  $\text{Fe}^{\text{III}}$  in intermediate X, 31.4 MHz.<sup>4</sup> However, the intrinsic value obtained for the smaller  $^{57}\text{Fe}$  tensor,  $|a_i| = 36.2$  MHz, is considerably larger than the respective intrinsic value reported for X,  $|a_i| = 25.3$  MHz.<sup>4</sup> This could indicate that center H may be better described as an  $\text{Fe}^{\text{III}}\text{Fe}^{\text{III}}$  center strongly coupled to a radical, as earlier suggested for intermediate X by Ravi et al.<sup>8</sup> These authors described a spin coupling model where the radical spin  $S = 1/2$  first couples to one  $\text{Fe}^{\text{III}}$  to form a  $S_i = 2$  or 3 intermediate spin, which then couples antiferromagnetically to the other  $\text{Fe}^{\text{III}}$  to form a  $S = 1/2$  ground state. In this model large spin projection factors can be calculated for both  $\text{Fe}^{\text{III}}$ , depending on the relative contribution of the two different intermediate spin states to the total spin in the ground state. For a pure  $S_i = 2$  or 3 intermediate spin state contribution the calculated spin projection factors are  $7/3$ ,  $-14/9$ ,  $2/9$  for  $S_i = 2$  and  $-5/3$ ,  $20/9$ ,  $4/9$  for  $S_i = 3$  for the three spin system  $\text{Fe}^{\text{III}}$  ( $S = 5/2$ ),  $\text{Fe}^{\text{III}}$  ( $S = 5/2$ ),  $\text{R}^{\bullet}$  ( $S = 1/2$ ).<sup>8</sup> The obtained intrinsic hyperfine values  $|a_i|$  for  $\text{Fe}^{\text{III}}$  and  $\text{Fe}^{\text{IV}}$  in center H, 29.8 and 31.05 MHz for  $S_i = 2$  and 31.3 and 29.0 MHz for  $S_i = 3$ , agree remarkably well with those for  $\text{Fe}^{\text{III}}$  in X, 31.4 MHz.<sup>4</sup> This model also explains the small anisotropy of the smaller hyperfine tensor of Fe1 in center H, which is more typical for  $\text{Fe}^{\text{III}}$  and too small for  $\text{Fe}^{\text{IV}}$ .

We therefore suggest that center H is an  $\text{Fe}^{\text{III}}\text{Fe}^{\text{III}}$  center with a strongly coupled, probably ligated radical. Possible candidates are a hydroxylated amino acid radical, or an oxygen derived ligand radical. Hydroxylation of F208 was observed in other mutants.<sup>9</sup> A phenoxyl type radical ligated to one of the irons could explain the stability of center H compared to X. Relatively stable phenoxyl ligand radicals have been reported for  $\text{Fe}^{\text{III}}$  model complexes.<sup>10</sup> In  $\text{H}_2\text{O}/\text{D}_2\text{O}$  exchange experiments we found a significant narrowing of the low-field side of the X-band EPR spectrum (not shown). Simulations of the spectra indicate that a large anisotropic hyperfine coupling of an exchangeable proton with tensor components up to 1.0 mT contributes to the spectrum of center H. The coupling could result from bridging or terminal OH or from water ligands of the irons. Large exchangeable hyperfine tensor components have been observed by ENDOR of MMO<sup>11</sup> and of X.<sup>12</sup> Such a large anisotropic coupling is, however, difficult to detect in the ENDOR spectra and we failed to observe it, probably due to the low yield of center H (3%). A more detailed report about mutagenesis, biochemical characterization, X-ray structure, and ligand ENDOR on R2-Y122H will be published in a forthcoming paper.<sup>7</sup>

**Acknowledgment.** We thank Prof. B. Hoffman, Dr. R. Bittl, and Dr. E. Bill for valuable discussion and Prof. B.-M. Sjöberg for advising us on the mutagenesis of R2-Y122H. This work was supported by DFG (La 751/3-1), the Strategic Nucleic Acid Research Programme, and the European TMR program (ERBFMRXCT98027).

JA0005892

(9) Logan, D. T.; deMaré, F.; Persson, B. O.; Slaby, A.; Sjöberg, B.-M.; Nordlund, P. *Biochemistry* **1998**, *37*, 10798–10807.

(10) Snodin, M. D.; Ould-Moussa, L.; Wallmann, U.; Lecomte, S.; Bachler, V.; Bill, E.; Hummel, H.; Weyhermüller, T.; Hildebrandt, P.; Wieghardt, K. *Chem. Eur. J.* **1999**, *5*, 2554–2565.

(11) DeRose, V. J.; Liu, K. E.; Kurtz, D. M., Jr.; Hoffman, B. M.; Lippard, S. J. *J. Am. Chem. Soc.* **1993**, *115*, 6440–6441.

(12) Willems, J.-P.; Lee, H.-I.; Burdi, D.; Doan, P. E.; Stubbe, J.; Hoffman, B. M. *J. Am. Chem. Soc.* **1997**, *119*, 9816–9824.

(13) (a) Lee, D.; Du Bois, J.; Petasis, D.; Hendrich, M. P.; Krebs, K.; Huynh, B. H.; Lippard, S. J. *J. Am. Chem. Soc.* **1999**, *121*, 9893–9894. (b) Dong, Y.; Que, L., Jr.; Kauffmann, K.; Münck, E. *J. Am. Chem. Soc.* **1995**, *117*, 11377–11378.